특 집

MEMS 기술과 정보기기 및 가전사업

박 재 영, 부 종 욱
LG전자기술원 마이크로시스템그룹

I. Introduction

A MEMS technology enabling the batch fabrication of miniaturized mechanical structures, devices, and systems has been originated from the Integrated Circuit (IC) technology. But it has now established enough of its own unique characteristics due to its diverse applications and distinctive natures of its market. Though MEMS technology had started from the silicon planar technology or more specifically from the silicon based sensor technology of the 1960s, noticeable advances in the technology and development of infrastructure has occurred in the 1990s. The remarkable research achievements during the last decade and the potential for MEMS technology to be one of the most promising and commercially viable one in the next century are well recognized. Thus, the technology will play important roles in consumer electronics over the nest five to 10 years. In particular, the key application areas to give the greatest impact will be microdisplays using micromirror arrays, mass/nano storage including hard disk drives/optical drives, RF/optical switching products, and sensing products such as accelerometers and IR/pressure sensors.

In this paper, RF MEMS research is discussed as a key application of the MEMS technology in consumer electronics. The main stream in the next generation of mobile/wireless communications such as celluar/PCS, PDA, and IMT 2000 is to develop and utilize smaller, lighter, cheaper, and secure systems with various functionality, low power consumption, and operation at muti-band/mode. These new systems will be able to provide high speed wireless internet, PC communication, wireless communication, MPEG file transmission, banking, and micro PC with the same function as a notebook or desk top computer. Thus, these components and systems are being developed with new technologies and concepts in many mobile communication companies. The MEMS is being recognized as a core technology to give the greatest impact in constructing the nextgenerationofmobile/wirelesscommunication products. The micromachine technology also enables the mass production of these micro RF devices or systems through their batch fabrication. A single chip communication transceiver, one of the key elements in the wireless/mobile communication system, can be realized by fabricating micro-scaled RF components with good performance characteristics and to partially/fully integrate MMICs or RFICs with the newly developed RF MEMS components by using the micro-machine technology.

II. RF MEMS Components for Single Chip Transceiver

⟨Figure 1⟩ shows the system level schematic drawing for a typical wireless transceiver. There are a large number of RF MEMS components can be served as fundamental building blocks for constructing an integrated single chip transceiver, including RF mechanical switches, tunable capacitors, high Q inductors, high Q resonators, RF filters, micro antennas, low lossy transmission lines, and etc. RF components and modules fabricated in the basis of current state-of-the art circuit designs using a combination of many GaAs FETS, PIN diodes, and varactors in order to achieve the required switching, filtering, and tuning functions have the disadvantages of high power consumption, low reliability, and high manufacturing cost. RF MEMS is a core technology that addresses these shortcomings and offers the better performance advantages. The following subsections now describe important RF MEMS components capable of miniaturizing, integrating, and improving their performance.

1. RF MEMS switches

So far, semiconductor switches such as FETs or PIN diodes are widley used in millimeter wave integrated circuits (MMICs) and microwave circuits. However, these semiconductor switches have large insertion loss and poor isolation in

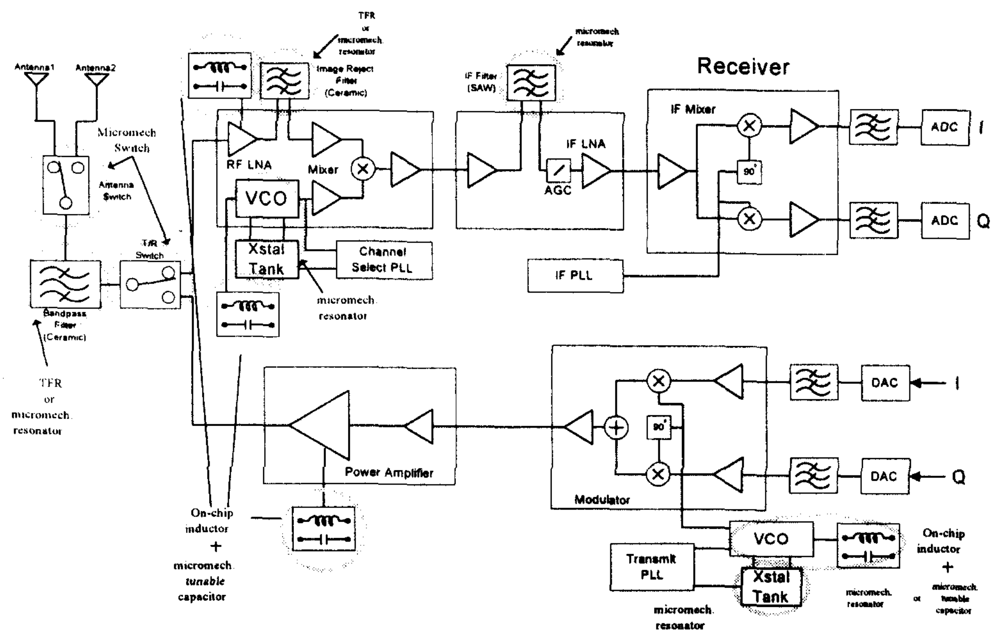

⟨**Figure 1**⟩ A system level schematic drawing for a typical wireless transceiver the 'ON' state and 'OFF' state at high frequency operation. The semiconductor switches have also large resistive loss, power consumption, and low power handling capability. Some semiconductor switches, such as silicon FETs, can handle a high level of signal power at low frequency, but the performance drops off dramatically as operating frequency increases. Others, such as GaAs metal semiconductor field effect transistors (MESFETs)[1-2] and PIN diodes[3], work fairly well at high frequency, but handle minimal signal power level. Accordingly, new switching elements have been demanded for substituting these semiconductor switches.

Recent development in MEMS technology has made possible the design and fabrication of micromechanical switch as a new switching element. The micromechanical switches have low resistive loss, negligible power consumption, good isolation, and high power handling capability compared to the semiconductor switches. RF MEMS switches have also integration compatibility with electronics with batch fabrication.

Mcromechanical switches were among the first devices studied in the RF MEMS field. In early 1979, a membrane-based RF MEMS switch was fabricated on silicon[4]. Since then, a large number of RF MEMS switches with electrostatic actuation designs[5] including cantilevers[6-10] and multiple-supported or membrane structures[6,11-16] have been investigated. Common applications of these RF MEMS switches include signal routing, impedance matching networks, arrayed capacitor banks, phase shifters, adjustable gain

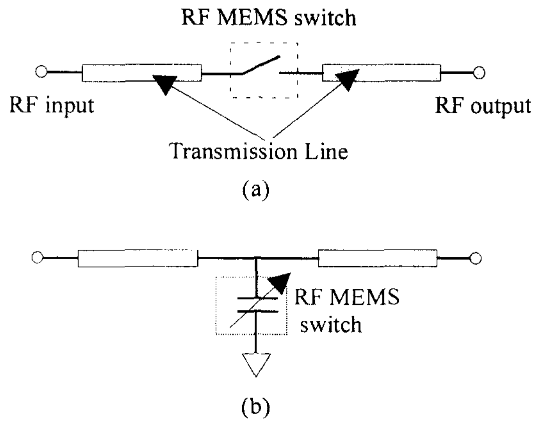

〈**Figure 2**〉 A schematic drawing of metal contacting serial switch configuration (a) and capacitive coupling shunt switch configuration (b)

amplifiers, and etc.

The RF MEMS switches can be distinguished as two types of switches based on the working principle such as metal contacting[6] and capacitive coupling[13]. The switches can also be divided into two types such as serial and shunt, as shown in 〈Fig. 2〉. Most of metal contacting switches is used as the serial switch configurations, while capacitive coupling switches are often used as the shunt switches. The metal contacting switches are to use metal-to-metal direct contact to obtain an ohmic contact between two electrodes, as illustrated in 〈Fig. 2〉. The MEMS metal contacting switch covers the broad frequency range, but it has a shorter contact lifetime than the capacitive coupling switches. Rockwell Science Center (RSC) fabricated MEMS metal contact switch by using surface micromachining techniques on the GaAs wafer[6,11]. The fabricated device has a device size of 80×160 um, actuation voltage of less than 60 V, insertion loss of 0.2 dB at dc to 40 GHz, and

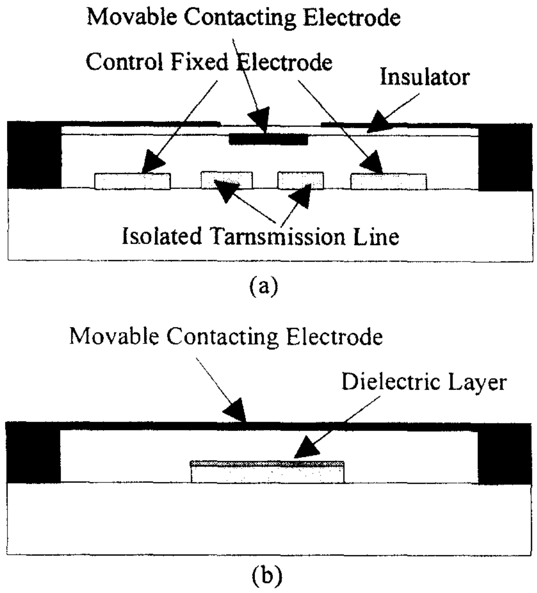

〈Figure 3〉 A cross-sectional view of shematic drawing of RF MEMS metal contacting resistive (a) and capcitve coupling capctive switches (b)

isolation of 32 dB at 10 GHz. In the MEMS metal contacting switches, the contact material should be selected based on considerations of the contact resistance, metal sticking behaviour, life time, and environmental and packaging compatibility.

As shown in 〈Fig. 3〉, the MEMS capacitive coupling switches have a thin dieleçtric film and an air gap between the two metal electrodes. Silicon nitride or oxide is commonly used as a dielectric layer in the capacitive RF MEMS seitches. The capacitive switches control mechanically an electrical current or signal by using the on/off impedance ratio, while resistive switches utilize the mechanical connection of two isolated transmission lines. Thus, high capacitance on/off ratio is desirable for achieving the high impedance ratio of the switches. When a voltage is applied between the movable plate and the transmission line of the capacitive switches shown in 〈Fig. 3〉, the electrostatic force pulls the movable plate down onto the dielectric layer. The dielectric layer can reduce stiction and eliminate microwelding between the movable plate and the transmission line. When the switch is off or unactuated, the off capacitance can be calculated by using the following equation:

$$C_{off}=\frac{1}{\dfrac{h_{dielectric}}{\varepsilon_{dielectric}\,\varepsilon_0 A}+\dfrac{h_{air}}{\varepsilon_0 A}} \tag{1}$$

When the switch is on or actuated, the on capacitance can be obtained by using the following equation:

$$C_{on}=\frac{\varepsilon_{dielectric}\,\varepsilon_0 A}{h_{dielectric}} \tag{2}$$

Thus, the off/on ratio of the RF MEMS capacitive switch can be approximately calculated by using the following equation:

$$\frac{Z_{off}}{Z_{on}}=\frac{C_{on}}{C_{off}}=\frac{\varepsilon_{dielectric}\,h_{air}+h_{dielectric}}{h_{dielectric}} \tag{3}$$

The theoritical cutoff frequency of the capacitive switch can be calculated by using the following equation where the ratio of off and on impedance degrades to unity:

$$f_{cutoff}=\frac{1}{2\pi R_{on}C_{off}} \tag{4}$$

The actuation voltage of the micromechanical switch can be determined by the applied voltage, the hinge geometry, the membrane material properties, and the gap height between the movable plate and dielectric layer on top of the transmission line. A first order solution of the pull-down

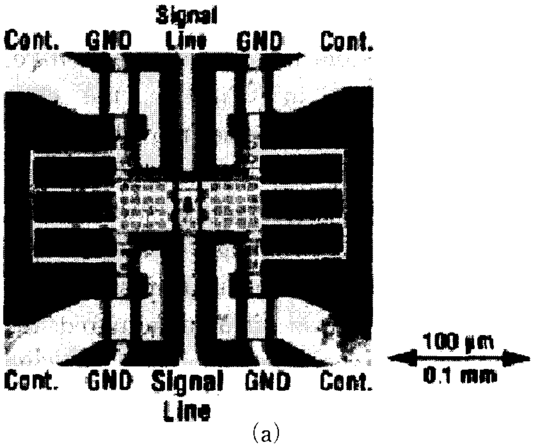

(a)

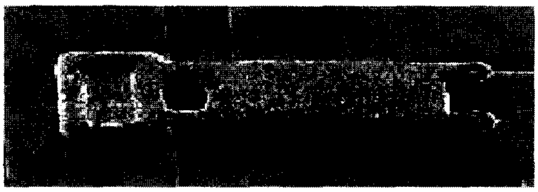

(b)

〈**Figure 4**〉 SEM pictures of metal contacting restive RF MEMS switches f (from RSC (a) and Northeastern University (b))

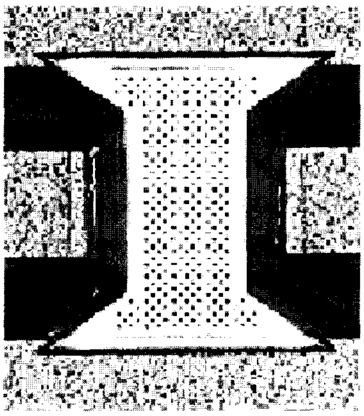

〈**Figure 5**〉 A photomicrographof capacitve coupling capacitive RF MEMS switch (form Texas Instrument)

voltage(V_P) can be calculated by the following equation[14]:

$$V_p=\sqrt{\frac{8K_s g_0^3}{27\varepsilon_0}} \tag{5}$$

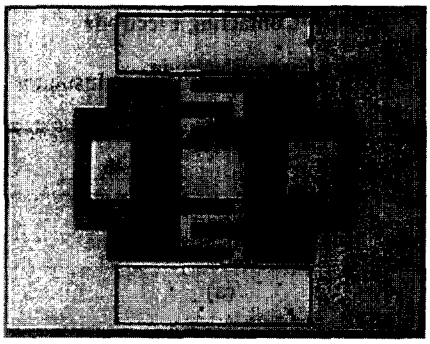

(a)

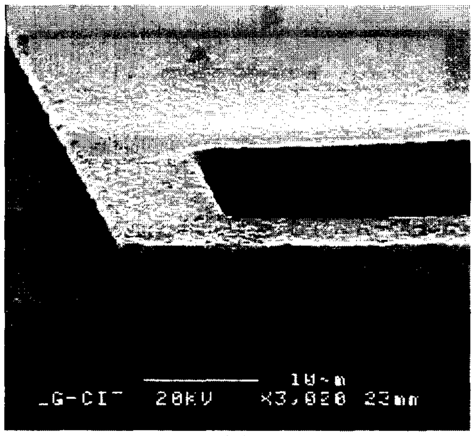

(b)

〈**Figure 6**〉 (a) A photomicrograph and (b) a close up view of capacitve coupling capacitive RF MEMS switch (from LG Electronics Institute of Technology)

where K_s is the spring constant of the mechanical system, g_0 is the initial gap between the movable electrode and the fixed electrode.

Texas Instrument (TI) developed RF MEMS shunt capacitive switch on high resistivity silicon wafer by using surface micopmching technique[13-15]. The switch has dimensions of 120 μm in width and 280 μm in length, and consists of a thin aluminum alloy membrane suspended over a dielectric film deposited on top of the bottom electrode. In the membrane up state, most of the RF signal passes through the transmission line with a minimal capacitance C_{off} of 35 fF between the bottom signal line and the suspended movable top electrode. When an electrostatic voltage of 50 V is applied between the movable top electrode and the bottom electrode, an electrostatic force is created to pull, the top electrode moves down onto the dielectric film on top of the bottom electrode. This configuration increases the coupling capacitance C_{on} between the signal line and the grounded membrane to 2.1~3.5 pF, resulting in an on-off capacitance ratio approximately between 60 and 100. Thus, high impedance ratio is desirable for achieving better switching characteristics in the capacitive RF MEMS switches. Silicon nitride or oxide commonly used may not be appropriate for making RF MEMS capacitive switches with small size, high on capacitance, and high on/off ratio due to their small relative dielectric constant at high frequencies. Thus, LG Elite utilized the STO with high dielectric constant for fabricating RF MEMS capacitive switches[17]. The fabricated switches have low insertion loss of less than 0. 1 dB, high on/off ratio of 500, high isolation of 40 dB at 2 GHz, and low operation voltage of 7.5 volts.

The most important parameter of the RF MEMS switches to be commercialized is the switch lifetime, which is often measured in a number of different ways depending on the requirements of the targeted applications. It is distinguished cold-switched and hot-switched lifetime. Cold-switching refers to the opening and closing of a switch with zero signal level through the contact, while hot-switching refers to that of a switch with a specified signal level through the contact. Thus, a switch lifetime can differ a great deal based on different switching conditions. For general RF applications, the measurement of hot-switched lifetime is necessary with a certain RF signal level passing through the contact.

2. Tunable Capacitors

The tunable capacitors or varactors are widely used components in RF communications due to its tuning functionality. They can be utilized in various applications including harmonic frequency generators, low noise parametric amplifiers, and frequency controllers such as

〈**Table 1**〉 Comparison of performance characteristics of the electrostatic RF MEMS switches fabricated by using surface micromachining technique

Parameters	GaAs FET	RSC	TI	HRL	Michigan	LG Elite
Actuation voltage (V)	~ 1	~ 60	~ 50	~ 25	15 ~ 20	5 ~ 10
Insertion loss (dB)	2 at 6 GHz	0.2	0.15 at 10 GHz	0.2	0. 6 at 22 GHz	~ 0.1
Isolation (dB)	22 at 2 GHz	32 at 10 GHz	15 at 10 GHz	40 at 12 GHz	20 at 22 GHz	42 dB at 5 GHz
Switching time (us)	0.01	2 − 5	3.5 − 5.3	20	−	5 − 10
Contact mechanism		Au metal	capacitive	Au metal	capacitive	

voltage controlled oscillators. There are important parameters to be evaluated of the tunable capacitors such as unbiased base capacitance, tuning ratio, equivalent series resistance or Quality factor, self-resonant frequency, and device linearity in response to RF power. The value of the unbiased base capacitance depends on the circuit requirements of a specific application and typically the useful values range from 0. 1pF to a few picoFarads for RF applications. The tuning ratio is a parameter that is often found to be a limiting factor in RF circuit design. In most applications, large tuning ratio in excess of 2 : 1 is demanded. The Q factor can be calculated by using the following equation (6) since other loss factors are negligible compared to resistive loss caused by the equivalent series resistance.

$$Q=\frac{1}{\omega CR} \tag{6}$$

As shown in the above equation, when the resistance is larger, the quality factor is smaller. Thus, the equivalent series resistance should be low enough to achieve high Q of the tunable capacitor. The series inductance in the equivalent circuit of the tunable capacitor should be also low enough to achieve high electrical self resonant frequency. Since the series inductance, together with the capacitance, will resonate at a frequency known as the electrical self-resonance. In most applications the tunable capacitor is required to have an extremely high linearity in response to RF signal power. Since a solid-state varactor has a large dependence on the signal power, multiple varactor devices are often used in a parallel-series configuration to increase the overall linearity. Although the parallel-series configuration of the varactors behaves similar to one single varactor in terms of capacitance tuning, the increased number of the components cause the issues in reliability, cost, size, weight, and power consumption.

In summary, the solid-state varactors often suffer from a small tuning ratio, excessive resistive loss, a low Q caused by large series resistance, and low self resonant frequency due to the large parasitic effects from the silicon substrate. Recently MEMS based high performance tunable capacitors are realized. These MEMS tunable capacitors tune their capacitance by adjusting device physical dimensions such as the varying the gap between top and bottom electrodes or the overlapping capacitive area based on the interdigitated comb structures.

In 1996, a gap tuning capacitor developed by using a surface micromachining tech-

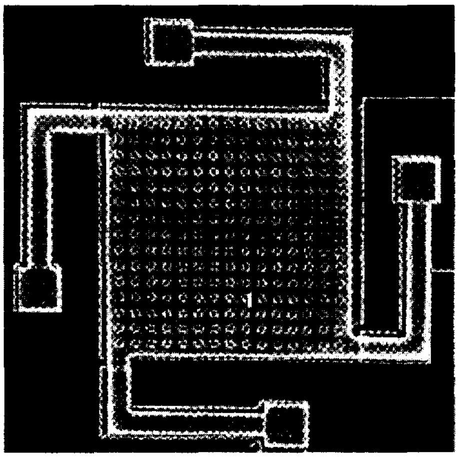

〈**Figure 7**〉 A photomicrograph of RF MEMS tunable capacitor with gap tuning configuration (from University of California at Berkeley)

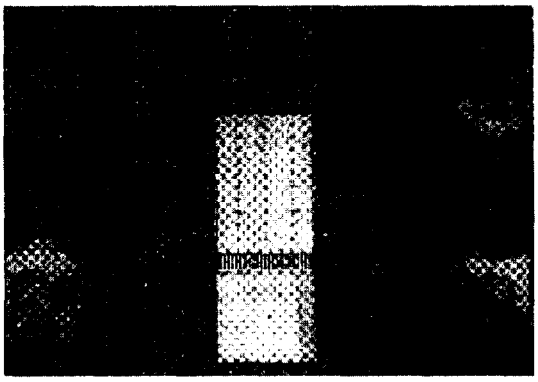

〈**Figure 8**〉 A photomicrograph of RF MEMS tunable capacitor with gap tuning configuration (from University of Colorado)

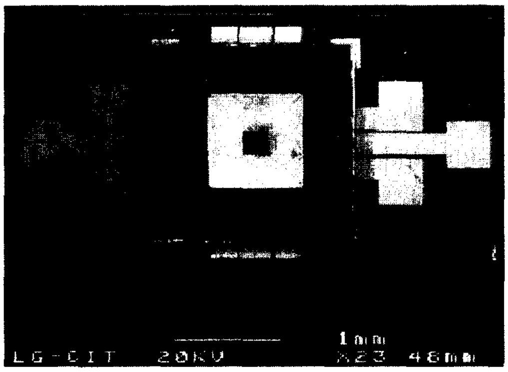

(a)

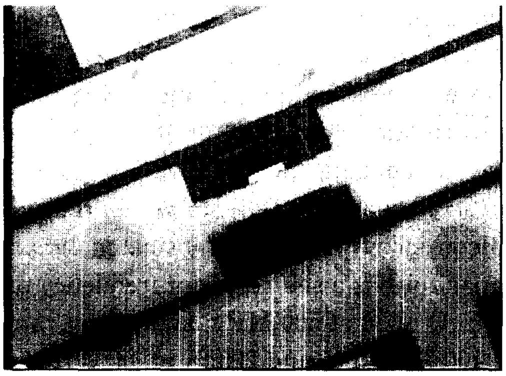

(b)

〈**Figure 9**〉 A photomicrograph of RF MEMS tunable capacitor with gap tuning configuration: (a) picture was taken at the front side and (b) picture was taken at the backside (from LG Electronics Institute of Technology)

nique[18]. As shown in 〈Fig. 7〉, the top electrode of the tunable capacitor supported by mocromachined springs, is moved in the vertical direction over the bottom electrode by electrostatic force as applying the tuning voltage between the electrodes. In this tunable capacitor, thick aluminum (1um) was used as the electrodes to reduce the resistive loss and the thick oxide layer (4um) was used to reduce parasitic effects as an insulating layer between the silicon substrate and devices. The tunable capacitor comprised of the electrode size of 200×200 um and the gap height of 1, 5um has the performance characteristics such as a tuning range of 16% at 5.5 V, the equivalent series resistance of 1.2 ohm at 1 GHz, and the quality factor of 62. In the tunable capacitors with electrostatically actuated two parallel plate system, their operations are limited within one-third of the initial gap due to the equilibrium condition between the electrostatic attracting force and the spring back force of the compliant. Thus, this imposes a theoretical limit of 50% on the capacitance tuning range. In 1997 the tunable capacitor comprised of three-plate parallel plate system was developed to increase the theoretical MTR (maximum tuning range) limit from 50% to 100% using a multi-user MEMS polysilicon process (MUMPs)[19]. In 1999, the tunable capacitor using electro-thermal actuator was fabricated by using MUMPs process and then flip-chip assembled onto an alumina substrate[20]. The device has a tuning ratio of 100% with a tuning voltage of 5 V and the quality factor of 256 at 1 GHz for the 0.102 pF, and the self resonant frequency

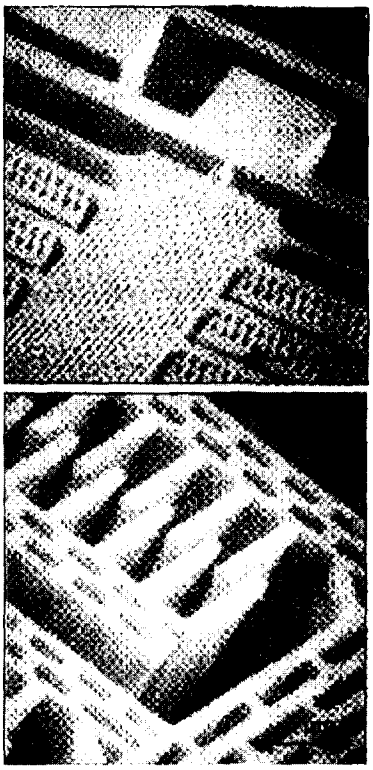

〈**Figure 10**〉 (a) A SEM picture and a close up view of RF MEMS tunable capacitor with area tuning configuration (from Rockwell Science Center)

of 31 GHz. In 2001, the RF MEMS tunable capacitor using piezoelectric actuator was fabricated on a Quartz substrate[21]. It has a tuning ratio of approximately 200% at 6 volts and quality factor of 210 at 1 GHz. The electrostatically actuated RF MEMS tunable capacitors described in the above can be easily integrated with other conventional electronics. However, as the capacitor is tuned higher on capacitance, RF breakdown in the capacitor air gap is more likely to occur.

In 1998, a MEMS area tuning capacitor based on integrated comb structures using a deep reactive ion etch (DRIE) of single-crystal silicon which is later coated with metal film[22]. One set of the comb structures is stationary and the other movable. When a tuning voltage is applied across the interdigitated comb structures, the electrostatic force of the comb fingers laterally actuates the movable portion of the device, resulting in a change of the overlapping area in the capacitor structure. However, the gap between the comb finger electrodes remains unchanged. Unlike the gap-tuning parallel plate tunable capacitors, there is no theoretical tuning limit for the tunable capacitors with area-tuning interdigitated comb structures. The only practical limits for the tuning range are related with the supporting spring design and the length of the comb fingers. 〈Fig. 10〉 shows the fabricated tunable capacitors with a large area of comb fingers, 2um in width, 2 um in spacing, 20-30 um in height, and supporting spring of 1mm in length and same width and height as the come fingers. These tunable capacitors were fabricated, characterized, and compared on a low resistivity silicon, a high resistivity silicon, and a glass substrate. The tunable capacitor has better performance fabricated on glass substrate due to reducing the resistive loss and the substrate parasitic effects compared with silicon substrates. The fabricated tunable capacitor has a self resonant frequency of 5 GHz, Q of 34 at 500 MHz, and tuning range of 100 % at 5 V and 200 % at 14 V respectively. The total capacitance per unit area for a comb structure heavily is dependent on the aspect ratio of the comb fingers.

〈**Table 2**〉 Comparison of performance characteristics of the RF MEMS tunable capacitors fabricated by using surface micromachining technique

Parameters	Solid-state varactors	RSC	U of Colorado	HRL	U of Cal. at Berkeley	LG Elite
Actuation voltage (V)	~ 4	2 – 14	~ 5	80 – 200	~ 5.5	~ 6
Min. capacitance (pF)	2 at 4 V	1.8	0.9	0.035	2.11	0.1
Tuning range (%)	335	200	~ 90	185	16	200
Quality factor	350 at 0.05 GHz	34 at 0.5 GHz	256 at 1 GHz	–	62 at 1 GHz	210 at 1 GHz
Actuation mechanism	Hyperabrupt junction	Electrostatic	Electro-thermal	Sliding motor	Electrostatic	Electro-piezoel.

3. High Q Inductors

Integrated inductors with high performance are in increasingly higher demands in modern wireless communications products. They can be utilized in various applications including filters, oscillators, low-power converters, and RF front ends of wireless transceivers. Key parameters in the integrated inductors are the quality factor Q, inductance, and the self-resonance frequency that the device transforms from inductive to capacitive characteristics. Resistive metal lines and dielectric losses in the substrate are mainly contributing to degrading the quality factor and inductance of the integrated inductors. The self resonant frequency is limited by various fringing and parasitic capacitance between windings and a substrate. The quality factor of integrated inductors on silicon substrate was ranged 1 to 10, while that of integrated inductors suspended on the substrate was ranged from 10 to 50. So far, the integrated inductor with the highest quality factor of 140 was a large suspended spiral inductor with thick copper coil on a glass substrate fabricated by using surface machining techniques and polymer/metallic process[23].

Much research has been done to improve the performance characteristics of integrated inductors by reducing resistive metal lines, parasitics, and dielectric losses from the substrate. Recent examples include air gap spiral inductor structures that have been fabricated using glass microbump bonding (GMBB) to reduce losses and parasitic capacitance[24]. Due to the presence of the air gap, the parasitic capacitance can be minimized, thereby enhancing the resonant frequency. A large suspended inductor on silicon for RF amplifier applications was fabricated in[2]; the deleterious effects of the silicon substrate were reduced by selectively etching out the silicon under the inductor. Transistor-integrated suspended spiral inductors formed from the metallization used in GaAs technologies have been produced; using air-bridge technologies, these devices have a typical air gap of 3 m between the conductor lines which form the inductor and the substrates[26]. Solenoid-type inductors have also been produced using a combination of electroplating and micromachining techniques that are suspended approximately 20 m above the substrate[27]. Examples of integrated passive filters incorporating integrated inductors have also been presented. A thin film LC passive filter has been fabricated by RF sputtering and ion-milling techniques[28]. A multilayer thin-film air core passives filter for the 850 MHz band was demonstrated in[29].

For high frequency applications, it is most appropriate to consider air-core inductor devices, since the high frequency behavior of many magnetic core materials is relatively poor. The characteristics of integrated inductors with a non-magnetic core can be determined solely by the coil geometry and location. In addition to accurate determination of the inductance of air-core inductors, it is also important at high frequency to assess parasitic effects such as stray capacitance and conductor skin effect in order to understand the effective operation of the device. Much research has been done to analyze the stray capacitance of an integrated inductor in high frequency applications[30-32]. The stray capacitance of the inductor determines the self resonant frequency (SRF) and the Q-factor. Various aspects of the inductor geometry, such as the cross-sectional area of the conductor line, the line spacing, and the core size, must be considered such that the inductor has the desired performance after fabrication. The resistivity of the metal conductor should be low to obtain a high Q-factor at high frequency applications. Since high frequency current flows mostly along the surface area of a conductor, the skin effect causes the winding resistance to increase as the frequency is increased. Thickness of conductor lines much in excess of several skin depths at the frequency of interest will not greatly reduce the conductor resistance or increase the inductor Q-factor.

Much research has been performed for modeling spiral inductors and predicting their inductance with and without consideration of parasitic effects[33-35]. As shown in Equation (7), a square spiral inductor may be defined by the 5 independent geometric variables in free space[36]:

$$L=F(D+d,\ D-d,\ N,\ s,\ t) \qquad (7)$$

where D and d are the outermost and innermost dimensions, and N, s, and t are the number of turns, line spacing and metal thickness of the given square spiral inductor. Bryan found an empirical equation to calculate the inductance of a flat square spiral-type inductor based on these variables[35,37]:

$$L=0.0241aN^{(5/3)}\ln[8(a/c)] \qquad (8)$$

where:

$$a=\frac{D+d}{4},\ c=\frac{D-d}{2} \qquad (9)$$

The above equation (2) predicts induct ance in microhenries when dimensions are expressed in centimeters. The unloaded Q-value is found by taking the ratio of the imaginary part to the real part of the input impedance of the inductor (neglecting bonding pads and interconnect) as shown in the following equation:

$$Q_{unloaded}=\frac{\mathrm{Im}\{Z_{in}\}}{\mathrm{Re}\{Z_{in}\}} \qquad (10)$$

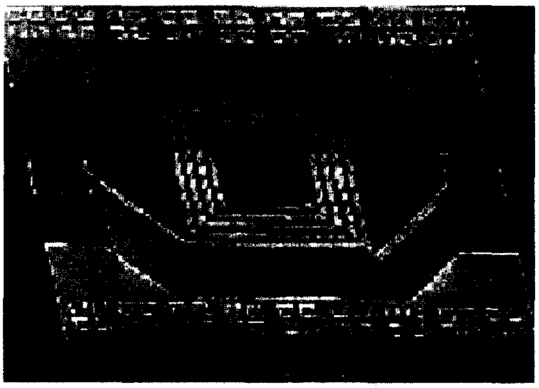

〈**Figure 11**〉 A SEM picture of integrated high Q spiral inductors suspended on a silicon substrate

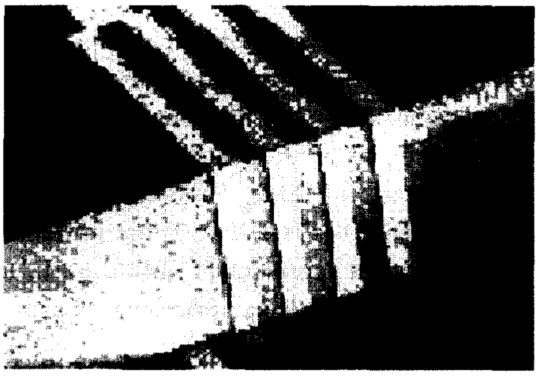

〈**Figure 12**〉 A SEM picture of solenoid type copper coil inductor with an alumina core (from University of California at Berkeley)

High quality factor means that the inductor has the desirable properties of low dissipation and favorable frequency characteristics when utilized in filter circuits.

〈**Figure 13**〉 A SEM picture of integrated solenoid type copper coil inductor suspended on an alumina substrate (from Georgia Institute of Technology)

〈**Figure 14**〉 A SEM picture of integrated spiral type copper coil inductor suspended on an glass substrate (from LG Electronics Institute of Technology)

4. T0hin Film Bulk Acoustic Resonators

Recent development of wireless communication technology demands the miniaturized on-chip RF filters with high performance characteristics, small volume, and light weight. However, the conventional methods using lumped elements, dielectric resonators, or surface acoustic wave resonators have serious difficulties in fabrication and integration[38] with other electronics. A thin film bulk acoustic resonator (TFBAR)[39] is a promising candidate for fabricating integrated RF filters, RF duplexers, and voltage controlled oscillators (VCOs), because the FBAR can be easily scaled down and integrated with other electronics. And also it has high quality factor (Q) in the wide spectral range from 0.1 GHz to 10 GHz[40-41] and better power handling characteristics compared to the SAWs, especially at high frequencies where the pitch of the interdigitated structures must be reduced. The TFBAR can be distinguished as membrane type resonator and solidly mounted resonator based on the fabricated structure configurations. The membrane type device is a resonator fabricated on top of supported nitride, silicon, or oxide membrane formed by etching the substrate selectively, while the SMR is a resonator fabricated on top of multiple reflectors formed on the substrate. The reflector is comprised of alternating low and high mechanical impedance materials to have large reflection and reduce the substrate impedance to near zero. In SMR type, energy loss to the substrate is avoided by acoustically isolating the substrate from the piezoelectric resonator materials using impedance transformations obtained through strategic selection of the number and thickness of layers separating the two media. A vibration or resonance is created by expansion and contraction of the piezoelectric layer, when an alternating electrical potential is applied across the TFBAR with a structure of metal-piezoelectric material-metal, as shown in 〈Fig. 16〉. AlN and ZnO is widely used as a piezoelectric material for fabricating RF TFBARs due to their high acoustic velocity, low dielectric constant, low acoustic loss, and high acoustic coupling factor at high frequency. As depicted in Equation (11), a resonant frequency, f_r can approximately be determined by the thickness of piezoelectric material.

$$2fr = n(h/v_p + d/v_m) \qquad (11)$$

where h is a thickness of piezoelectric layer, d is a thickness of metal electrode, V_p is a propagation velocity of acoustic wave in piezoelectric material, and V_m is a propagation velocity of acoustic wave in metal electrode. With all of their advantages, there are still several important drawbacks such as trimming and tuning, when these resonators are utilized to implement small percent bandwidth filters. Recently, Agilent developed the miniaturized TFBAR duplexer for US PCS handset. It is less than 2 mm in thickness and has a footprint of only 5.6×11.9 mm^2. It has good performance characteristics such as power handling of 30 dBm, insertion loss of 2.2 dB and noise blocking of 42 dB at 1930 1990 MHz, and insertion

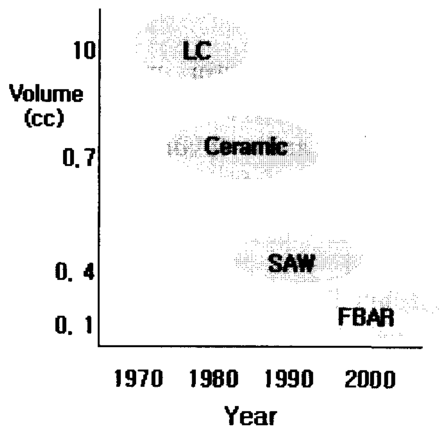

〈Figure 15〉 A trend of RF filters used in RF applications based on their volume loss of 1.8 dB and interferer blocking of 54 dB at 1850 − 1910 MHz.

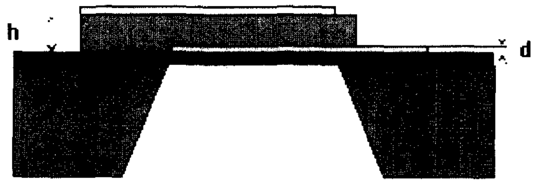

〈**Figure 16**〉 A cross-sectional view of membrane type thin film bulk acoustic resonator (TFBAR):metal electrode-piezoelectric layer-metal electrode-membrane structure

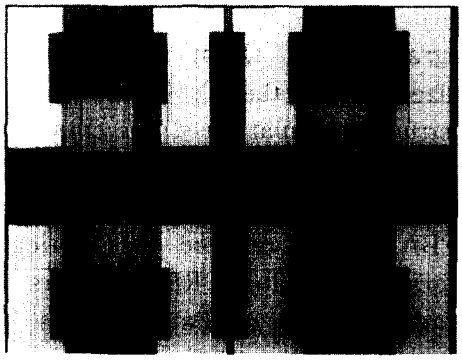

〈**Figure 17**〉 A photomicrograph of fabricated 4 TFBARs on a silicon nitride membrance (from LG Elite)

〈**Table 3**〉 Recent history of TFBARs and TFBAR filters research

Parameters	**Westing house**	**Motorola**	TFR	**Agilent**	**RSC**	**LG Elite**
Resonator type	membrane	membrane	SMR	Membrane	SMR	membrane
Piezoelectric materials	ZnO	ZnO	AlN	AlN	ZnO	AlN/ZnO
Filter type	ladder	lattice	ladder	Ladder	ladder	ladder

Ⅲ. Conclusions

The recent progress in RF MEMS for wireless and mobile communication applications was reviewed in this paper. The RF MEMS devices reviewed include micromechanical switches, tunable capacitors, integrated high Q inductors, and thin film bulk acoustic resonators to become core components for constructing miniaturized transceivers operated at multi-band and multi-mode. The micromechanical switches, the first devices studied in the RF MEMS field, are widely being developed due to their low resistive loss, negligible power consumption, good isolation, and high power handling capability compared to the semiconductor switches. The RF MEMS switches having integration compatibility with other electronics can be utilized as well switching elements as tuning elements. The solid-state varactors suffer from small tuning ratio, poor device linearity, excessive resistive loss, low Q caused by large series resistance, and low self resonant frequency due to the large parasitic effects from the silicon substrate. Thus, MEMS based high performance tunable capacitors are being realized to overcome the shortcomings of these solid-state varactors. These MEMS tunable capacitors tune their capacitance by adjusting device physical dimensions such as the varying the gap between top and bottom electrodes or the overlapping capacitive area based on the interdigitated comb structures. They can be utilized in various applications including harmonic frequency generators, low noise parametric amplifiers, matching networks, and frequency controllers such as voltage controlled oscillators. Large suspended integrated high Q microinductors are realized by using the MEMS technology for constructing miniaturized one chip filters, oscillators, and low-power converters. A thin film bulk acoustic resonator (TFBAR) was realized for fabricating integrated RF filters, RF duplexers, and voltage controlled oscillators (VCOs) with high performance characteristics, small size/volume, and light weight, because the FBAR can be easily scaled down and integrated with other electronics. A miniaturized single chip communication transceiver, one of the key elements in the wirelee/mobile communication system, can be realized by fabricating micro-scaled components with good performance characteristics and to partially/ fully integrate MMICs or RFICs with the newly developed RF MEMS components by using the micromachine technology.

For the RF MEMS technology being successful and commercialized, the RF MEMS technologies and components should be well developed and their commercialization should be promoted in the first phase. In the second phase, partially integrated modules and systems comprised of the fabricated RF MEMS components and RFICs should be developed and their commercialization should be promoted. In the third phase, the fully integrated modules and systems like a single chip transceiver should be developed and their commercialization should be promoted. In order to ensure continued success of the RF MEMS in the commercial arena, several key issues also need to be addressed. The industry standards in fabrication process and reliability should be established, and the infrastructure should be also built and shared.

Acknowledgment

This work has been partially supported by Ministry of the Ministry of Science & Technology under 21st Frontier Intelligent microsystem Project. We would like to acknowledge valuable contributions from many colleagues at microsystem group of Materials and Devices laboratory in the LG Electronics Institute of Technology.

References

〔1〕 Gopinath A and Rankin J B, “GaAs FET RF switches,” *IEEE Trans. Electron Devices* **32** 1272-8, 1985

〔2〕 Ota Y, Sakakura M, Fujimoto K, Yamamoto S and Fujimoto H, “High isolation and low insertion loss switch IC using GaAs MESFET’s”, *IEEE Trans. Microwave Theor. Technol.* **43** 2175-7, 1995

〔3〕 Kobayashi K W, Oki A K, Umemoto D K, Claxton S K Z and Streit D C, “Monolithic GaAs HBT p-I-n diode variable gain amplifiers, attenuators, and switches *IEEE Trans. Microwave Theor. Techniq.* **41** 2295-302, 1993

〔4〕 Petersen K E, “Micromechanical membrane switches on silicon,” *IBM J. Res. Dev.* **23** 376-85, 1979

〔5〕 Gr’etillat M-A, Gr’ etillat F and de Rooij N F, “Micromechanical relay with electrostatic actuation and metallic contacts," *J. Micromech. Microeng.* **9** 324-31, 1999

〔6〕 Yao J J and Chang M F, "A surface micromachined miniature switch for telecommunications applications with signal frequencies from DC up to 4 GHz," *Tech. Digest, 8th Int. Conf. on Solid-State Sensors and Actuators* pp. 384-7, 1995

〔7〕 Schiele I, Huber J, Evers C, Hillerich B and Kozlowski F, "Micromechanical relay with electrostatic actuation," *Tech. Digest, Int. Conf. on Solid-State Sensors and Actuators* pp.1165-8, 1997

〔8〕 Hyman D *et al*, "Surface-micromachined RF MEMS switches on GaAs substrates," *Int. J. RF Microwave CAE* **9** 348-61, 1999

〔9〕 Hyman D *et al*, "GaAs-compatible surface-micromachined RF MEMS switches," *Electron. Lett.* **35** 224-6, 1999

〔10〕 Suzuki K, Chen S, Marumoto T, Ara Y and Iwata R, "A micromachined RF microswitch applicable to phased-array antennas," *Tech. Digest, IEEE Microwave Theory Techniques Symp.* pp.1923-6, 1999

〔11〕 Sovero E A, Mihailovich R, Deakin D S, Higgins J A, Yao J J, DeNatale J F and Hong J H, "Monolithic GaAs PHEMT MMICs integrated with high performance MEMS microrelays," *Proc. IMOC'99 (Rio de Janeiro, Brazil)*, 1999

〔12〕 Muldavin J B and Rebeiz G M, "30 GHz tuned MEMS switches," *Tech. Digest, IEEE Microwave Theory and Techniques Symp.* pp.1511-14, 1999

〔13〕 Goldsmith C, Lin T-H, Powers B, Wu W-R and Norvell B, "Micromechanical membrane switches for microwave applications," *Tech. Digest, IEEE Microwave Theory and Techniques Symp.* pp.91-4, 1995

〔14〕 Goldsmith C, Randall J, Eshelman S, Lin T-H, Denniston D, Chen S and Norvell B, "Characteristics of micromachined switches at microwave frequencies," *Tech. Digest, IEEE Microwave Theory and Techniques Symp.* pp.1141, 1996

〔15〕 Yao Z J, Chen S, Eshelman S, Denniston D and Goldsmith C, "Micromachined low-loss microwave switches," *IEEE J. MEMS* 8 129-34, 1999

〔16〕 Pacheco S, Nguyen C T and Katehi L P B, "Micromachined electrostatic K-band switches," *Tech. Digest IEEE MTT-S Int. Microwave Symp.* pp. 1569-72, 1998

〔17〕 Jae Y. Park, Geun H. Kim, Ki W. Cheong, and Jong U. Bu, "Electroplated RF MEMS Capacitive Switches, *IEEE 13th International MEMS Conference*, Miyajaki, Japan, January, pp. 639-644, 2000

〔18〕 Young D J and Boser B E, "A micromachined variable capacitor for monolithic low-noise VCOs," *Tech. Digest, Solid State Sensor and Actuator Workshop* pp.86-9, 1996

〔19〕 Dec A and Suyama K, "Micromachined varactor with wide tuning range," Electron. Lett. **33** 922-4, 1997

〔20〕 Harsh K F, Zhang W, Bright V M and Lee Y C, "Flip-chip assembly for Si-based RF MEMS," *Proc. IEEE, 12th*

Ann. Int. Workshop on Micro Electro Mechanical Systems pp.273-8, 1999

[21] Jae Y. Park, Young J. Yee, Hyo J. Nam, and Jong U. Bu, "Micromachined RF MEMS Tunable Capacitors using Piezoelectric Actuators," *Tech. Digest, IEEE Microwave Theory and Techniques Symp. May*, 2001

[22] Yao J J, Park S and DeNatale J, "High tuning-ratio MEMS-based tunable capacitors for RF communications applications," *Tech. Digest, Solid State Sensor and Actuator Workshop* pp.124-7, 1998

[23] Jae Y. Park and Mark G. Allen, "Micromachined High Q Inductors for High Frequency Applications", *Micromachining & Microfabrication '98 Conference, SPIE*, vol. 3514, pp.218-228, Santa Clara, CA 1998

[24] J. Chuang, S. Ghazaly, N. Zein, G. Maracas, and H. Gronkin, "Low loss air-gap spiral inductors for MMICs using glass microbump bonding techniques", *IEEE-MTT-S International Microwave Symposium Digest*, vol. 2, pp.131-133, 1998

[25] J. Y. C. Chang, A. A. Abidi, and M. Gaitan, "Large suspended inductors on silicon and their use in a 2 μm CMOS RF amplifier", *IEEE Electron Devices Letters*, vol. 14, no. 5, May 1993

[26] M. E. Goldfarb and V. K. Tripathi, "The effect of air bridge height on the propagation characteristics of the microstrip", *IEEE Microwave Guided Wave Letter*, vol. 1, pp.273-274, Oct. 1991

[27] Y. J. Kim and M. G. Allen, "Surface micromachined solenoid inductors for high frequency applications", *IEEE Transactions on Component, Packaging, and Manufacturing Technology (Part-C)*, vol. 21, no. 1 p.26-33, Jan. 1998

[28] M. Yamaguchi, K. Ishihara, and K. Arai, "Application of thin-film inductors to LC filters", *IEEE Transactions on Magnetics*, vol. 29, no. 6, pp.3222-3225, 1993

[29] V. Sadhir, I. Bahl, and D. Willems, "CAD compatible accurate models of microwave passive lumped elements for MMIC applications", *International Journal of Microwave and Millimeter-Wave Computer-Aided Engineering*, vol. 4, no. 2, pp.148~162, 1994

[30] A. Massarini, M. Kazimierczuk, and G. Grandi, "Lumped parameter models for single-and multiple-layer inductors", *27th Annual IEEE Power Electronics Specialists Conference*, vol. 1, pp.295-301, 1996

[31] G. Grandi, M. Kazimierczuk, A. Massarini, and U. Reggiani, "Stray capacitances of single-layer air-core inductors for high-frequency applications", IAS'96. *IEEE Industry Applications Conference*, pp.1384-8 vol. 3, 1996

[32] B. Breen, "Multi-layer inductor for high frequency applications", *41st Electronic Components and Technology Conference*, pp.551-4, 1991

[33] D. Cahana, "A new transmission line approach for designing spiral microstrip inductors for microwave integrated circuits", *IEEE-MTT-S International Microwave Symposium Digest*, pp.245-247, 1983

〔34〕 W. O. Camp, S. Tiwari, and D. Parson, "2-6 GHz monolithic microwave amplifier", *IEEE-MTT-S International Microwave Symposium Digest*, pp. 46-49, 1983

〔35〕 H. M. Greenhouse, "Design of planar rectangular microelectronic inductors", *IEEE Trans. Parts, Hybrids and Packaging*, vol. PHP-10, pp. 101-109, June 1974

〔36〕 Ping Li, "A new closed form formula for inductance calculation in microstrip line spiral inductor design", *Electrical Performance of Electronic Packaging*, pp. 58-60, 1996

〔37〕 H. Bryan, "Printed inductors and capacitors", *Tele-Tech & Electronic Industries*, PP. 68, 1955

〔38〕 R. B. Strokes and J. D. Crawfold, "X- and thin film acoustic filters on GaAs," IEEE Tran. Microwave Theory Tech., vol. 41, pp. 1075~1080, July 1993

〔39〕 S. H. Kim, J. S. Lee, H. C. Choi, and Y. H. Lee, "The Fabrication of Thin-Film Bulk Acoustic Wave Resonators Employing a ZnO/Si Composite Diaphragm Structure Using Porous Silicon Layer Etching," IEEE Electron Device Letter, vol. 20, NO. 3, March 1999

〔40〕 K. M. Lakin, G. R. Kline, and K. T. McCarron, "High Q Microwave Acoustic Resonators and Filters," Proceedings of the 1993 IEEE MTT-S International Microwave Symposium, vol. 5, pp. 1517~1520, 1993

〔41〕 W. W. Lau, Y. Song, and E. S. Kim, "Lateral-Field-Excitation Acoustic Resonators For Monolithic Oscillators and Filters," IEEE International Frequency Control Symposium, pp. 558~562, 1996

저 자 소 개

朴 宰 永

1971년 4월 1일생, 1997년 12월 Ph. D. at Electrical and Computer Engineering in the Georgia Institute of Technology, 1997년 12월~1999년 2월 : Research Engineer in Georgia Tech. 1999년 12월~현재 : Research at LG 전자기술원, 〈주관심 분야 : optical, RF, and Bio MEMS

부 종 욱

He received the Ph. D. degree in Metallurgical Engineering from Korea University 1992. He has been with LG Corporate Institute of Technology, Seoul, Korea since 1984, where he has worked on the area of silicon micromachining and microsensors. From 1995 to 1996, he has been with the Center for Integrated Sensors and Circuits, Department of Electrical Engineering and Computer Science, University of Michigan, Ann Arbor, as a visiting scholar. Currently, he is a group leader with Microsystem team in LG Corporate Institute of Technology.

His research interests include development of microfabrication and micromachining technologies for microsystem; IR sensors, optical communication components, RF MEMS, MEMS embedded high density data storage systems, and biomedical applications. He has published and presented more than 70 papers